

Depletion of Centromeric MCAK Leads to Chromosome Congression and Segregation Defects Due to Improper Kinetochore Attachments^D ^V

Susan L. Kline-Smith,* Alexey Khodjakov,[†] Polla Hergert,[†] and Claire E. Walczak^{‡§}

Departments of *Anatomy and Cell Biology and [‡]Biochemistry and Molecular Biology, Indiana University Medical Sciences Program, Bloomington, Indiana 47405; and [†]Laboratory of Cell Regulation, Division of Molecular Medicine, Wadsworth Center, Albany, New York 12201-0509

Submitted August 11, 2003; Revised November 20, 2003; Accepted November 21, 2003
Monitoring Editor: Lawrence Goldstein

The complex behavior of chromosomes during mitosis is accomplished by precise binding and highly regulated polymerization dynamics of kinetochore microtubules. Previous studies have implicated Kin Is, unique kinesins that depolymerize microtubules, in regulating chromosome positioning. We have characterized the immunofluorescence localization of centromere-bound MCAK and found that MCAK localized to inner kinetochores during prophase but was predominantly centromeric by metaphase. Interestingly, MCAK accumulated at leading kinetochores during congression but not during segregation. We tested the consequences of MCAK disruption by injecting a centromere dominant-negative protein into prophase cells. Depletion of centromeric MCAK led to reduced centromere stretch, delayed chromosome congression, alignment defects, and severe missegregation of chromosomes. Rates of chromosome movement were unchanged, suggesting that the primary role of MCAK is not to move chromosomes. Furthermore, we found that disruption of MCAK leads to multiple kinetochore–microtubule attachment defects, including merotelic, syntelic, and combined merotelic-syntelic attachments. These findings reveal an essential role for Kin Is in prevention and/or correction of improper kinetochore–microtubule attachments.

INTRODUCTION

Accurate chromosome segregation is crucial to maintain genomic integrity; thus, the cell has devised a complex macromolecular machine called the mitotic spindle to control this process. The spindle is made up of a bipolar array of microtubules (MTs) extending from opposing spindle poles to chromosomes at the spindle equator. MTs are structurally polar polymers with the “minus” ends located at spindle poles and the more dynamic “plus” ends free to search three-dimensional space to attach to chromosomes. Chromosomes are connected to spindle MTs via kinetochores, which are specialized proteinaceous structures localized in the outer layer of the centromere on each sister chromatid. Ultrastructural analyses of the vertebrate kinetochore have established that this organelle is comprised of an electron-dense inner plate, which is proximal to the inner centromeric chromatin, and an outer plate, which attaches to a bundle of MTs often called the K-fiber (Rieder, 1982).

After the nuclear envelope has broken down, sister kinetochores of a chromosome aid in establishing biorientation on the spindle by coming into contact with and stabilizing MTs from both spindle poles (McIntosh *et al.*, 2002). As

chromosomes make more attachments to dynamic MTs from opposing spindle poles and move toward the spindle equator, increased tension is generated across sister kinetochores. The amount of tension is reflected in the physical distance between opposing kinetochores, which is maximal at metaphase when chromosomes have achieved a full complement of MTs at each kinetochore (~25 MTs in vertebrate somatic cells; McEwen *et al.*, 1997). Elegant cytological analyses of somatic cells suggest that kinetochores generate a pulling force by depolymerizing the plus ends of the attached kinetochore MTs. This pulling force, in combination with the coupling activity of kinetochore-associated motor proteins, is largely responsible for the chromosome movement necessary for congression of chromosomes to the metaphase plate and segregation of chromatids at anaphase A (Inoue and Salmon, 1995). Both tension and MT attachment at the kinetochore are thought to be important in a kinetochore-dependent mitotic checkpoint that delays anaphase until all chromosomes are properly aligned (McIntosh *et al.*, 2002, Musacchio and Hardwick, 2002; Zhou *et al.*, 2002).

Given the chance encounters with MTs experienced by kinetochores in early mitosis, it is not surprising that improper attachments do arise (Nicklas, 1997). Both meiotic and mitotic systems have demonstrated various maloriented attachments, which can include a single kinetochore making attachments to both spindle poles (merotelic) and both kinetochores making attachments to a single pole (syntelic). In addition, electron microscopic (EM) analysis has shown that MTs can penetrate past the outer plate of the kinetochore, and nonkinetochore MTs occasionally invade the inner centromeric region of a chromosome (Rieder, 1982). In mitotic

Article published online ahead of print. Mol. Biol. Cell 10.1091/mbc.E03-08-0581. Article and publication date are available at www.molbiolcell.org/cgi/doi/10.1091/mbc.E03-08-0581.

^D ^V Online version of this article contains supplementary figures and video material. Online version is available at www.molbiolcell.org.

[§] Corresponding author. E-mail address: cwalczak@indiana.edu.

systems, many of these attachments are unstable and are corrected before and/or during anaphase by unknown mechanisms (Rieder and Salmon, 1998; Cimini *et al.*, 2003); however, some of these problems, such as merotelic attachments, are not sensed by the mitotic checkpoint machinery in cultured cells (Cimini *et al.*, 2001, 2002). This suggests the cell may have backup methods by which to correct such improper kinetochore–MT attachments during mitosis.

In this report, we have focused on the role of mitotic centromere-associated kinesin (MCAK) (Wordeman and Mitchison, 1995) in kinetochore–MT attachments and progression through mitosis. MCAK belongs to a unique group of kinesins, the Kin Is, which depolymerize MTs rather than translocate along them (Desai *et al.*, 1999; Hunter *et al.*, 2003; Ovechkina and Wordeman, 2003). The localization of MCAK at the centromere and its activity as a MT depolymerase make it an excellent candidate for a regulator of K-fiber dynamics and/or a destabilizer of incorrect kinetochore–MT attachments. MCAK centromere dominant-negative constructs cause lagging chromosomes at anaphase in Chinese Hamster Ovary (CHO) cells (Maney *et al.*, 1998), as well as chromosome misalignment in metaphase-arrested *Xenopus* egg extracts (Walczak *et al.*, 2002). Loss of MCAK orthologues Klp5/6 in *Schizosaccharomyces pombe* results in defective chromosome movement and delayed mitosis (Garcia *et al.*, 2002; West *et al.*, 2002). Together, these data demonstrate that Kin Is are important for aspects of chromosome positioning, although it remains unclear how cells use a MT depolymerase at the centromere to ensure proper chromosome alignment and segregation. Therefore, we have performed detailed analyses of the mitotic defects ensuing from depletion of centromere-bound MCAK in cells. By using immunofluorescence, time-lapse phase contrast, and transmission EM, we reveal a new role for the MT depolymerase activity of MCAK in correction of both merotelic and syntelic maloriented attachments. In addition, this is the first demonstration for kinetochore–MT error correction by a kinesin-like protein, adding yet another important role for kinesins in maintaining the fidelity of chromosome segregation during mitosis.

MATERIALS AND METHODS

Cell Culture and Drug Treatments

PtK2 cells were grown in minimal essential medium α supplemented with 10% fetal calf serum, penicillin, streptomycin, and L-glutamine (Invitrogen, Carlsbad, CA) in a 37°C, 5% CO₂ incubator. *Xenopus* S3 cells (Cohen *et al.*, 2000) were obtained from Dr. Douglas DeSimone (University of Virginia, Charlottesville, VA) and were maintained at ~20°C in complete L-15 media at 70% supplemented with 10% fetal bovine serum and 1 mM sodium pyruvate (Invitrogen). For immunostaining, PtK2s were plated on 12-mm glass coverslips at 1/4–1/8 3–5 d before experimentation. S3s were plated on 12-mm glass coverslips at 1/2 3–4 d before experimentation. For time-lapse analyses, PtK2s were plated on 22 × 22-mm glass coverslips at 1/4–1/8 3–5 d before the experiment. All drugs were diluted in dimethyl sulfoxide (Sigma-Aldrich, St. Louis, MO). Nocodazole (Sigma-Aldrich) was used at 0.5 μ g/ml for 4 h or at 10 μ g/ml for 30–60 min, depending on the experiment. Paclitaxel (Sigma-Aldrich) was used at 10 μ M for 30 min. Monastrol, a gift from Dr. Tarun Kapoor (Rockefeller University, New York City, NY), was used at 100 μ M for 4–6 h.

Cloning, Expression, and Purification of Fusion Proteins

Fusion protein coding fragments were generated by polymerase chain reaction and inserted into the p6HisGFP vector (Walczak *et al.*, 2002). Green fluorescent protein (GFP)–CEN was constructed using the N-terminal domain of *Xenopus* MCAK (encoding aa 2–263) fused to a small portion of the C terminus (encoding aa 630–664) to increase stability of the purified protein. For control experiments, we generated a fusion construct (GFP') in which p6HisGFP was fused to the base pairs encoding aa 630–664. Constructs were verified by sequencing. DNA was transformed into BL-21s for protein expression. Protein expression and purification were carried out as described on our

Web site at (<http://php.indiana.edu/~walczak/pages/protocols.htm>). All fusion proteins were dialyzed into 10 mM HEPES, pH 7.2, 100 mM KCl, 25 mM NaCl, 50 mM sucrose, 0.1 mM EDTA, 0.1 mM EGTA. Quantification of fusion proteins was done by densitometry of Coomassie-stained gels by using bovine serum albumin as a standard.

Immunofluorescence

For analysis of kinetochore proteins, injected fusion proteins, and MTs, cells were rinsed in phosphate-buffered saline (PBS) (12 mM PO₄²⁻, 137 mM NaCl, 3 mM KCl, pH 7.4) and fixed for 20 min in PHEM (60 mM PIPES, 25 mM HEPES, 10 mM EGTA, 2 mM MgCl₂, pH 6.9) plus 4% formaldehyde prepared fresh daily. Fixed cells were rinsed with Tris-buffered saline-Triton X (TBS-TX) (20 mM Tris, 150 mM NaCl, pH 7.5, 0.1% Triton X-100) and blocked in AbDil (2% bovine serum albumin, 0.1% Na₂S₂O₃ in TBS-TX) for 30 min. TBS-TX was used for all subsequent rinses between antibody incubations. Antibodies were diluted in AbDil, and all incubations were 30 min, except for analysis of lagging chromosomes, for which cells were incubated overnight at 4°C in 1/500 CREST antibody, a gift from Dr. Bill R. Brinkley (Baylor College of Medicine, Houston, TX). For fluorescence of MTs, DMI α (Sigma-Aldrich) was used at 1/250. Anti-MCAK-NT (Walczak *et al.*, 1996) was used at 5 μ g/ml. Anti-hBubR1, a gift from Dr. Guowei Fang (Stanford University, Palo Alto, CA), was diluted 1/500. Anti-CENP-E, a gift from Dr. Tim Yen (Fox Chase Cancer Center, Philadelphia, PA), was diluted 1/4000. Cells were incubated for 30 min in the appropriate Texas Red or fluorescein isothiocyanate-conjugated secondary antibodies diluted 1/50–1/100 (Jackson ImmunoResearch Laboratories, West Grove, PA). To determine whether GFP-CEN inhibited the binding of endogenous MCAK to centromeres, we immunoadsorbed the anti-MCAK-CT antibody with a 10-fold molar excess of GFP' control fusion protein to remove the portion of the polyclonal antibody recognizing aa 630–664. As expected, this modified anti-MCAK-CT antibody did not recognize purified GFP-CEN or GFP' control protein, but it did recognize purified *Xenopus* MCAK by Western blot analysis (our unpublished data). DNA was visualized using 10 μ g/ml Hoechst in TBS-TX. Coverslips were mounted using 0.5% *p*-phenylenediamine, 20 mM Tris-Cl (pH 8.8) in 90% glycerol.

Microinjection

Microinjections were performed using a Nikon IM300 microinjector with Nikon/Narishige microinjector controls and a Nikon TE-300 inverted microscope. PtK2s were kept on a 37°C warming tray before microinjection in complete minimal essential medium α without phenol red, supplemented with 20 mM K-HEPES, pH 7.2. S3 cells were maintained at ~20°C in complete L-15 media. Injectate samples were spun at 90,000 rpm for 5 min to remove particulate matter and kept on ice during the experiment. GFP-CEN protein was injected at 50–100 μ M; control GFP' protein was injected at 150–300 μ M. For immunostaining experiments, microinjections were performed on 12-mm glass coverslips in a 35-mm tissue culture dish. Each coverslip was only injected for a period of 5 min and returned to the 37°C warming tray for PtK2 cells (or ~20°C for S3 cells) and then fixed at specific time points to analyze mitosis (30 min for mid-mitosis in PtK2s, 40 min for late mitosis in PtK2s/mid-mitosis in S3s, or 60 min for late mitosis in S3s). For time-lapse experiments, PtK2 cells were imaged using a Rose chamber (kindly provided by Dr. Edward Salmon, University of North Carolina, Chapel Hill, NC), which was covered with mineral oil and maintained at 35–37°C using an ASI air stream incubator (Nevtek, Burnsville, VA). Prophase cells were injected and allowed to recover for 1–3 min before imaging began. For correlative time-lapse phase contrast/fluorescence analysis of chromosomes, cells were plated on 12-mm coverslips mounted over a hole sealed with silicone grease in a 35-mm dish (Gorbsky and Ricketts, 1993). For correlative time-lapse phase contrast/electron microscopy, cells were plated on 12-mm grided coverslips (Eppendorf, Westbury, NY), which were mounted over a hole sealed with paraffin wax in a 35-mm dish.

Electron Microscopy

The ultrastructure of kinetochores in injected cells was analyzed by serial-section EM as described previously (Khodjakov *et al.*, 1997). Briefly, the samples were fixed in 2.5% glutaraldehyde in PBS, postfixed in 1% OsO₄, and embedded using standard protocols (Rieder and Cassels, 1999). Cells, previously followed by time-lapse phase contrast microscopy, were relocated after embedding via locator grids, and then serially thin sectioned (100 nm). Images were recorded on a Zeiss 910 microscope operated at 100 kV. The structure of the centromeric region was reconstructed by tracing profiles of chromosomes, kinetochores, and MTs in serial sections and then assembling three-dimensional (3-D) surface-rendered volumes in Stereon software (Marko and Leith, 1996).

Microscopy and Image Acquisition

For fluorescence microscopy, cells were imaged on a multimode time-lapse fluorescence microscope system similar to that described by Salmon *et al.* (1994). This system consists of a Nikon E-600 microscope equipped with a 100×/1.3 numerical aperture Plan Fluor oil objective (Nikon, Tokyo, Japan). Fluorescence images were collected digitally with a Micromax 1300 Y cooled

charge-coupled device camera (Roper Scientific, Trenton, NJ). For all immunofluorescence images, Z-series optical sections were obtained at 0.5- μm steps and then 3-D reconstructed with MetaMorph software (Universal Imaging, Downingtown, PA) and a stepping motor (Prior Scientific Instruments, Rockland, MD) unless otherwise stated in the text. Images in Figure 7 and Supplementary Figure 1 were deconvolved (blind iterative deconvolution) using Autodeblur 9.1 software (AutoQuant Imaging, Troy, NY). For time-lapse analyses, cells were imaged using a Nikon TE-300 inverted microscope equipped with a 40 \times /0.60 numerical aperture Plan Fluor objective (Nikon). Phase contrast microscopy images were collected digitally using a Cool Snap Cf camera (Roper Scientific) at 30-s or 15-s intervals, depending on the experiment. All cameras, shutters, and filter wheels were controlled by MetaMorph software. Micrographs were assembled in Adobe Photoshop for identical contrast enhancement, and montages were prepared using Adobe Illustrator.

Data Analysis

All linescan and distance measurements were made using MetaMorph software. Final processing of data and graphs was performed using Microsoft Excel. Analysis of chromosome and pole movement was performed similarly to Gordon *et al.* (2001). In MetaMorph, the distance from a chromosome to the spindle equator was measured for each frame of the time-lapse movie using the bulk of metaphase-aligned chromosomes as a reference point for the spindle equator. Pixel values were converted into actual distance measurements and chromosome movement was plotted using Excel. Chromosome movement was defined as P or AP when unidirectional movement occurred for $\geq 1 \mu\text{m}$. Values for chromosome behavior, such as velocities, number of switches in the direction of movement during oscillations, and timing in each direction of movement, were all determined in Excel. Data values are reported as mean \pm SEM. To determine significant differences between means, unpaired *t* tests assuming unequal variance were performed with significant differences considered when $p < 0.05$.

RESULTS

MCAK Displays Differential Localization to Centromeres throughout Mitosis

Previous studies reported the localization of XKCM1/MCAK at centromeres, at spindle poles, and in the cytoplasm in *Xenopus* XL177 cells (Walczak *et al.*, 1996) and CHO cells (Wordeman and Mitchison, 1995). For a more detailed analysis of centromere-bound MCAK, we coimmunostained PtK2 cells with anti-MCAK antibody and CREST, a human autoimmune antibody used to indicate the location of sister kinetochores (Figure 1). CREST serves as a marker for the inner region of the kinetochore and can be used to monitor the extent of centromere stretch (Waters *et al.*, 1996b; Hoffman *et al.*, 2001). We measured the length of MCAK staining across the centromere relative to CREST staining at sister kinetochores for all stages of mitosis (Table 1). MCAK began to accumulate at inner kinetochores in very early prophase. By mid- to late prophase, MCAK was localized across the centromere in a thick dumbbell shape or two closely spaced dots that overlapped with CREST staining, suggesting that MCAK extends from the inner centromere out to the inner plate of the kinetochore (Figure 1A). Once chromosomes began attaching to MTs, MCAK was decreased in the region of CREST (Figure 1B). This was especially evident during metaphase, where MCAK was stretched into a bar shape across the centromere, overlapping little with CREST (Figure 1C). On initiation of anaphase A, MCAK trailed behind CREST in a comet shape that may constitute the half-centromere that would remain after separation of sister chromatids (Figure 1D). By anaphase B and telophase, MCAK was completely colocalized with CREST (Figure 1, E and F). These results show that MCAK localization changes throughout mitosis and may be correlated with centromere stretch and/or MT attachment.

To examine how MCAK localization is affected by alterations in spindle dynamics, we treated cells with drugs that affect different aspects of the mitotic spindle. To reduce centromere stretch, cells were treated for 30 min with 10

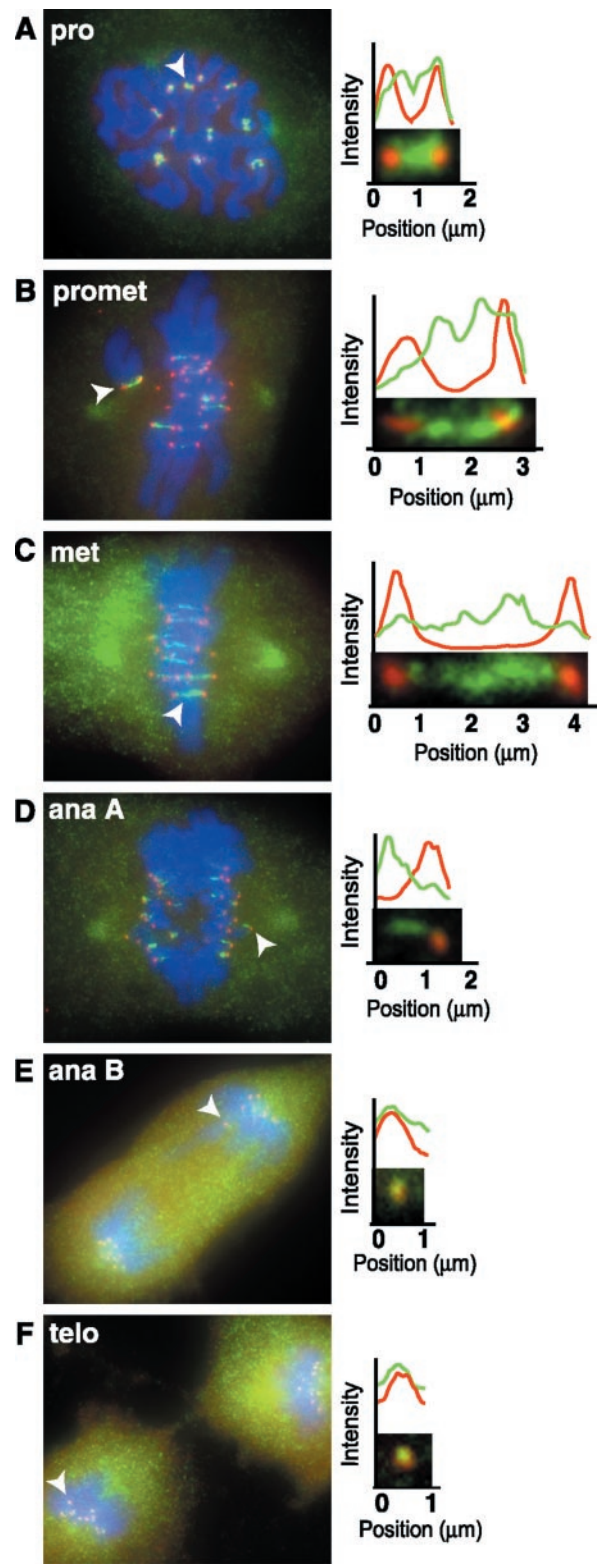


Figure 1. MCAK displays differential localization to centromeres throughout mitosis. (A–F, left column) PtK2 cells were fixed and stained for CREST (red), MCAK (green), and DNA (blue). To analyze the extent of colocalization of MCAK and CREST, line scans were generated in MetaMorph by drawing a two-pixel width line through centromeres for each stage of mitosis (A–F, right column). Centromeres used to generate line scans in this figure are denoted by solid arrowheads. Bar, 10 μm .

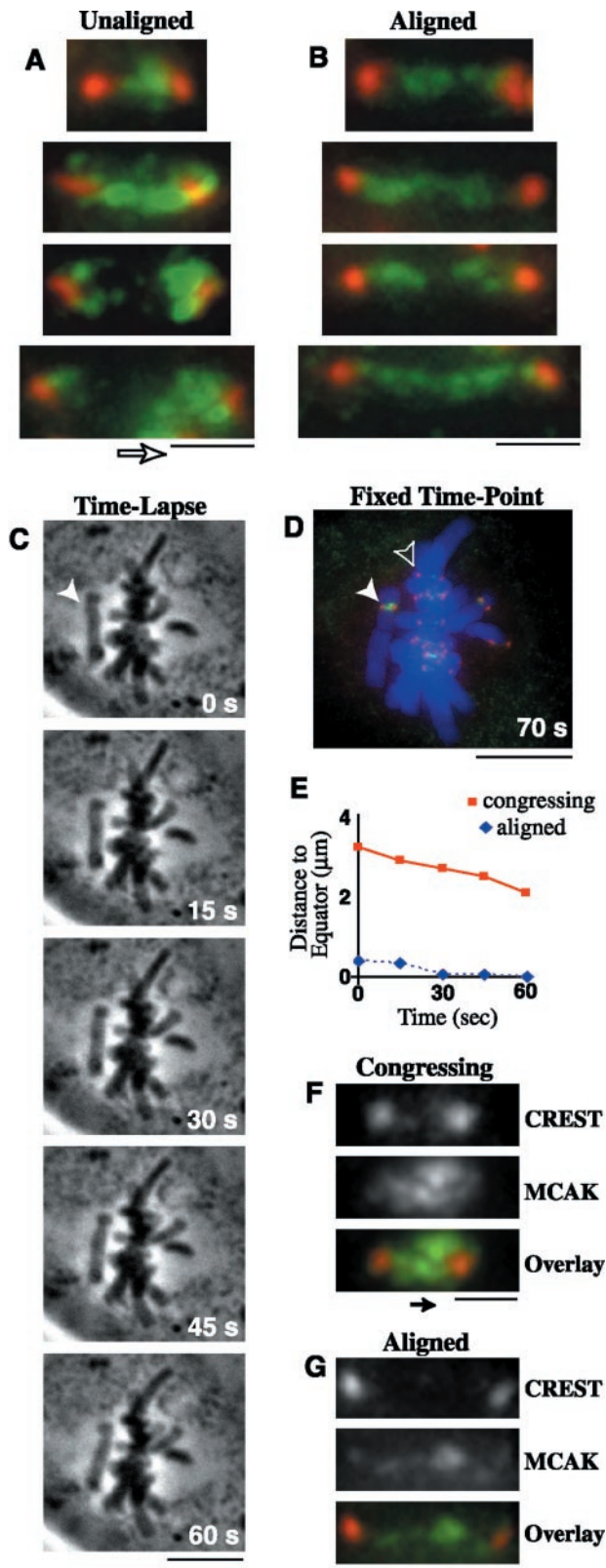


Figure 2. MCAK is enriched at the leading kinetochore of congressing chromosomes. PtK2 cells were fixed and immunostained for CREST (red), MCAK (green), and DNA (blue). (A) Centromeres of unaligned chromosomes exhibited increased levels of MCAK at the kinetochore facing the metaphase plate (direction indicated by open arrow), whereas (B) centromeres of aligned chromosomes

Table 1. Measurements of MCAK versus CREST localization at the centromere/kinetochore region

Mitotic stage	Interkinetochore distance of CREST	Length of MCAK staining at centromeres
	avg. $\mu\text{m} \pm \text{SEM}$ (n)	avg. $\mu\text{m} \pm \text{SEM}$ (n)
Prophase	1.34 ± 0.06 (22)	1.43 ± 0.06 (22)
Prometaphase		
Chrom at the pole	2.30 ± 0.13 (17)	2.31 ± 0.13 (17)
Bioriented chrom	3.27 ± 0.08 (77)	3.11 ± 0.09 (77)
Metaphase	3.81 ± 0.13 (27)	3.55 ± 0.14 (27)
Anaphase A	NA	1.23 ± 0.04 (53)

chrom, chromosomes; NA, not applicable.

Interkinetochore distances were determined by measuring the distance from the outer edge of CREST staining at one kinetochore to outer edge of CREST staining at its sister kinetochore versus the length of MCAK staining at centromeres. Sample sizes for all interkinetochore measurements are given in number of chromosomes.

$\mu\text{g}/\text{ml}$ nocodazole to destabilize MTs or $10 \mu\text{M}$ paclitaxel to stabilize MTs. We also treated cells for 4 h with $100 \mu\text{M}$ monastrol, which inhibits Eg5 activity, leading to monoastrial spindles with chromosomes exhibiting reduced centromere stretch (Kapoor *et al.*, 2000). All three treatments resulted in MCAK localizing to centromeres in a thick dumbbell shape or two closely spaced double dots overlapping with CREST, similar to the pattern observed in prophase (our unpublished data). We also treated cells with $0.5 \mu\text{g}/\text{ml}$ nocodazole for 4 h, which results in an expanded, crescent-like outer kinetochore region (De Brabander *et al.*, 1981; Hoffman *et al.*, 2001). Unlike CENP-E, a well-characterized outer kinetochore protein that displayed this characteristic crescent shape (Thrower *et al.*, 1996), MCAK exhibited a double dot staining pattern that colocalized with CREST, suggesting that MCAK is not a component of the outer kinetochore region (our unpublished data). Together, these findings suggest that MCAK localizes predominantly to the centromere (and thus farther from MT binding sites) under conditions of high centromere stretch; however, under conditions of reduced centromere stretch, MCAK localization approaches the kinetochore (and thus closer to MT binding sites).

MCAK Accumulates at the Leading Kinetochore of Congressing Chromosomes

We noticed that during prometaphase, unaligned chromosomes often had an accumulation of MCAK at the kinetochore facing the spindle equator (Figure 2A); however,

from the same cells showed an equal distribution of MCAK at both sister kinetochores. (C) Congressing chromosomes were analyzed by time-lapse phase contrast microscopy at 15-s intervals. Actual times are given in the lower right corner. White arrowhead indicates a chromosome moving to the metaphase plate for 1 min. (D) The cell shown in part C was fixed and immunostained to analyze a congressing chromosome (solid arrowhead), which exhibited motion toward the metaphase plate at $1.1 \mu\text{m}/\text{min}$ (E; solid red line), and displayed an increase in MCAK staining at the leading kinetochore (F; direction of motion indicated by the solid arrow). The aligned chromosome in D (open arrowhead), exhibited negligible motion at the metaphase plate (E; dashed blue line), and showed no difference in MCAK staining at either sister kinetochore (G). Bars (A, B, F, and G), $1 \mu\text{m}$; (C and D), $10 \mu\text{m}$.

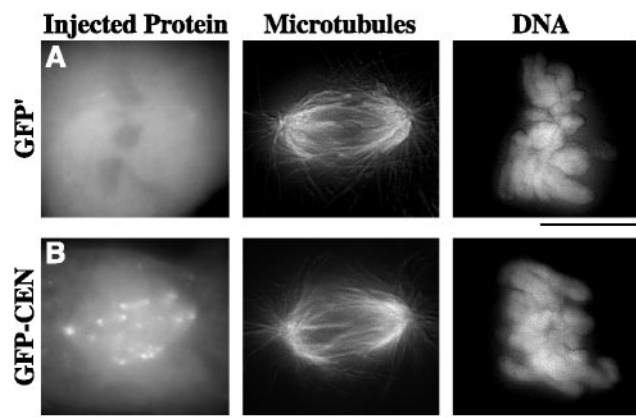


Figure 3. GFP-CEN binds kinetochores, centromeres, and spindle poles without disrupting global spindle morphology. PtK2 cells in prophase were injected with GFP' control (A) or GFP-CEN (B), the centromere dominant-negative version of MCAK. At 30 min postinjection, cells were fixed and immunostained for MTs and DNA. Bars, 10 μ m.

aligned chromosomes in the same prometaphase cells had an even distribution across the centromere (Figure 2B). This "accumulation" of MCAK was defined as an increase in the intensity, length, and/or width of MCAK staining at the kinetochore. We quantified the frequency of differential staining for unaligned chromosomes and found that MCAK was enriched at the kinetochore facing the metaphase plate on 56% ($n = 41$) of unaligned chromosomes, whereas 32% had no difference in staining between the two sister kinetochores. Only 12% of unaligned chromosomes had more MCAK localized to the sister kinetochore facing the spindle pole. These results suggest that MCAK might localize preferentially to the leading edge of a congressing chromosome, because the chromosomes located halfway between the spindle equator and the pole are usually exhibiting motion toward the spindle equator (our unpublished observations; Skibbens *et al.*, 1993). To test this idea, we used time-lapse phase contrast microscopy to image prometaphase cells with unaligned chromosomes (Figure 2C). When a chromosome exhibited at least 1 min of directed motion toward the metaphase plate (Figure 2E), the cell was immediately fixed. We then immunostained these cells for MCAK and CREST (Figure 2, D, F, and G) and quantified the frequency of differential MCAK staining at kinetochores. MCAK was enriched at the leading kinetochore in 67% ($n = 32$) of the congressing chromosomes; only one congressing chromosome had more MCAK staining at the trailing kinetochore. The remaining 31% of the congressing chromosomes showed no difference in MCAK staining at either kinetochore. These results reveal that MCAK preferentially localizes to the leading kinetochore of a congressing chromosome, which is the site exhibiting active MT depolymerization and decreased tension (McIntosh *et al.*, 2002).

GFP-CEN Depletes Centromere-bound MCAK without Affecting Bipolar Spindle Formation

To examine the role of MCAK in chromosome positioning, we constructed a fusion construct (GFP-CEN) between 6-his green fluorescent protein (GFP) and the N-terminal domain of *Xenopus* MCAK (aa 2–263) plus a small portion of the C terminus (aa 630–664) to enhance stability of the purified protein. The N terminus of MCAK has been shown to act as

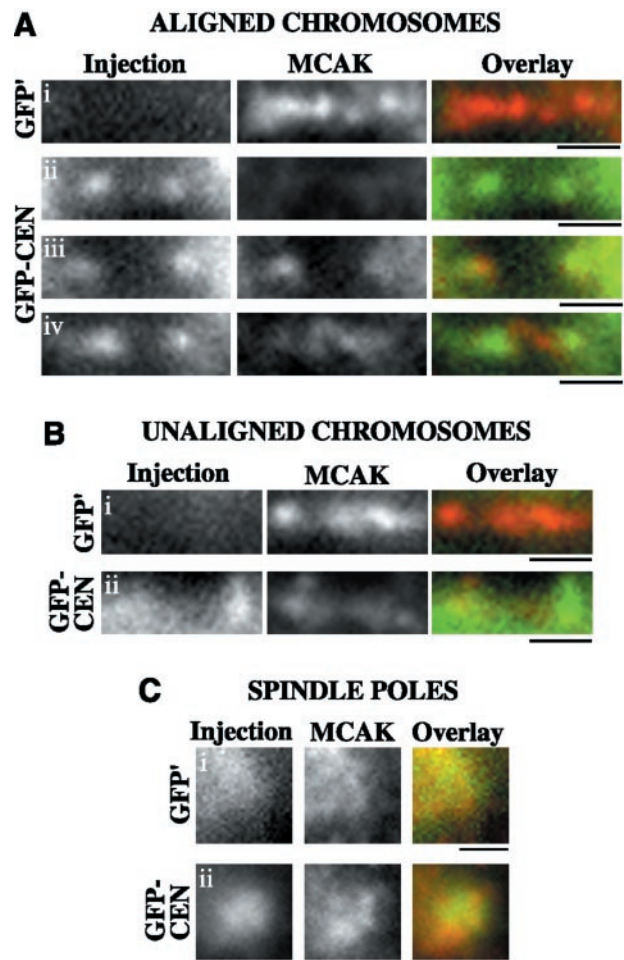


Figure 4. GFP-CEN depletes endogenous MCAK from centromeres but not from spindle poles. PtK2 cells in prophase were injected with GFP' control or GFP-CEN protein. At 30' postinjection, cells were fixed and stained to visualize endogenous MCAK (red) versus the injected proteins (green). Cells were analyzed by Z-series optical sectioning, and single plane images are shown. (A, i) Aligned chromosomes in GFP'-injected cells exhibited normal endogenous MCAK localization to the centromere. GFP-CEN binding at kinetochores inhibited endogenous MCAK from localizing to centromeres in the majority of cells (A, ii and iii), although a few aligned chromosomes retained a small amount of MCAK at the centromere (A, iv). Unaligned chromosomes in GFP'-injected cells exhibited intense localization of endogenous MCAK at the centromere (B, i), whereas GFP-CEN binding decreased the localization of MCAK (B, ii). Although both GFP' and GFP-CEN bound spindle poles during mitosis (C, i and ii), neither fusion protein disrupted MCAK localization to the spindle pole. Bars, 1 μ m.

a dominant-negative protein in egg extracts by displacing endogenous MCAK from kinetochores (Walczak *et al.*, 2002). The use of this dominant-negative construct would allow us to perturb centromere-bound MCAK without disrupting the cytoplasmic portion of MCAK, which is required for proper spindle formation and function (Walczak *et al.*, 1996; Kline-Smith and Walczak, 2002; Goshima and Vale, 2003). As a control for our dominant-negative construct, we created a fusion construct (GFP') between 6-his GFP and aa 630–664. We first tested these constructs in *Xenopus* egg extracts and found that GFP-CEN, but not GFP', bound to kinetochores in metaphase-arrested egg extracts (our unpublished data).

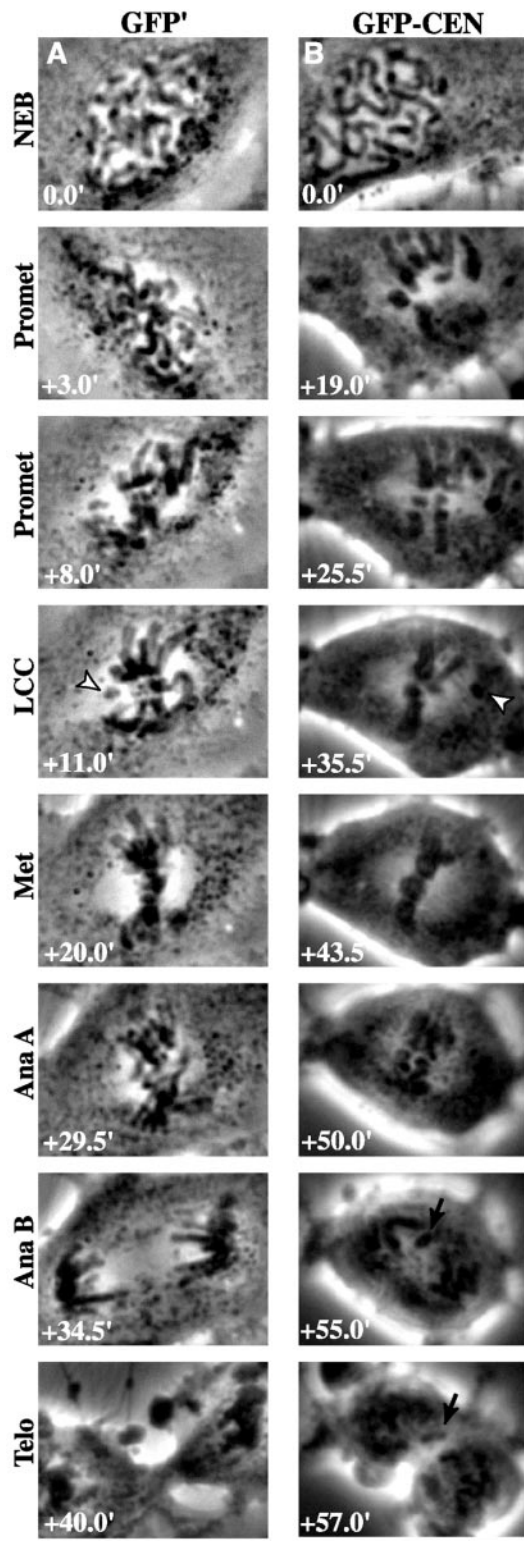


Figure 5. Depletion of centromere-bound MCAK perturbs chromosome alignment and segregation. PtK2 cells in prophase were injected with (A) GFP' or (B) GFP-CEN. Time-lapse phase contrast microscopy was used to image cells as they progressed through mitosis. The time for each stage of mitosis is given in minutes (bottom left), with NEB at $t = 0.0$ min. LCC is the time at which the last chromosome began congression (arrowheads). Note lagging chromatid (arrows) during anaphase B and telophase in B. Bar, 10 μ m.

To deplete centromere-bound MCAK in PtK2 cells, we injected GFP-CEN or control GFP' into the cytoplasm of prophase cells, because this is when MCAK first localizes to the kinetochore/centromere region. At 30 min postinjection, cells were fixed and processed for immunofluorescence of MTs and DNA (Figure 3). GFP-CEN targeted to kinetochores, centromeres, and spindle poles; however, the gross morphology of spindle MTs in these cells was normal, suggesting that the cytoplasmic pool of MCAK was not inhibited.

To characterize the association of GFP-CEN with the kinetochore/centromere region, we stained GFP-CEN-injected cells with CREST to analyze the localization of our dominant-negative fusion protein (Supplemental Figure 1). GFP-CEN was localized most intensely to the centromere and inner kinetochores of chromosomes under conditions of low tension (prophase, unaligned, and nocodazole). Aligned chromosomes also exhibited binding of GFP-CEN to inner kinetochores, whereas the localization of GFP-CEN at the centromere was variable. To address whether GFP-CEN inhibits the binding of endogenous MCAK to the centromere/kinetochore region, we stained injected cells with a polyclonal anti-MCAK antibody that recognizes endogenous MCAK but not the injected proteins (Figure 4). GFP'-injected cells displayed normal localization of endogenous MCAK binding at centromeres ($n = 16$ cells; Figure 4, Ai, and Bi). In contrast, GFP-CEN depleted endogenous MCAK from the centromeres of 71% of aligned chromosomes ($n = 14$ cells; Figure 4A, ii-iii), whereas 29% of aligned chromosomes exhibited some residual binding of MCAK at the centromere (Figure 4A, iv). Endogenous MCAK could still bind to centromeres on unaligned chromosomes, although this binding was reduced ($n = 4$ cells; Figure 4B, ii). The localization of endogenous MCAK to spindle poles, however, was not perturbed by GFP-CEN binding ($n = 18$ cells; Figure 4C, ii). These results show that the GFP-CEN fusion protein significantly inhibits the binding of endogenous MCAK to most centromeres, whereas the localization of MCAK to spindle poles is not perturbed. Because the polar and cytoplasmic pools of MCAK do not seem to be inhibited by GFP-CEN, this fusion protein allows us to specifically probe the defects resulting from depletion of MCAK from the centromere in cells.

Depletion of Centromere-bound MCAK Perturbs Chromosome Alignment and Segregation

To determine what aspects of mitosis were affected by the injection of GFP-CEN, we performed time-lapse analysis of mitosis in GFP-CEN-injected cells, GFP'-injected cells, and uninjected cells using phase contrast microscopy (Figure 5; Videos 1–3). Because no statistical differences were found between uninjected and GFP'-injected cells, all reported trends and statistics are comparing GFP-CEN- and GFP'-injected cells (Table 2). Cells injected with GFP-CEN took 9.4 min (31%) longer between nuclear envelope breakdown (NEB) and the onset of anaphase A. To distinguish congression defects versus deficiencies in the initiation of anaphase A, we determined the time at which the last chromosome began congressing (LCC) to the spindle equator (Shannon *et al.*, 2002). Injection of GFP-CEN led to a 9-min (67%) increase in the time between NEB and LCC; however, there was no difference in the amount of time between LCC and anaphase A. Thus, all of the mitotic delay exhibited by GFP-CEN-injected cells can be attributed to the delay in the initiation of chromosome movement toward the spindle equator. These results suggest that MCAK is required for proper congression of chromosomes.

Table 2. Analysis of mitotic progression in GFP' versus GFP-CEN-injected cells

Measurement	Control GFP'- injected cells	GFP-CEN-injected cells	Student's <i>t</i> test	Trends
	avg. \pm SEM	avg. \pm SEM		
Time between injection and NEB (min)	15.9 \pm 3.4	12.4 \pm 1.3	<i>p</i> = 0.35	No difference
Time between NEB and LCC (min)	13.5 \pm 1.1	22.5 \pm 2.5	<i>p</i> < 0.01	9.0 min (67%) increase
Time between LCC and Ana A (min)	16.7 \pm 1.1	17.1 \pm 1.7	<i>p</i> = 0.98	No change
Total time between NEB and Ana A (min)	30.2 \pm 1.3	39.6 \pm 1.9	<i>p</i> < 0.001	9.4 min (31%) increase
Sample size (no. cells)	15	18		

NEB, nuclear envelope breakdown; LCC, time at which the last unaligned chromosome initially attempted to congress; Ana A, time at which sister chromatids first began to segregate.

Mitotic progression was analyzed in cells injected with control GFP' fusion protein or GFP-CEN.

We next analyzed the behavior of chromosomes in cells injected with GFP-CEN (Table 3). Chromosomes in these cells had difficulties congressing to the metaphase plate, with 50% of cells exhibiting a high preponderance of chromosomes lingering at poles (Figure 5B; Videos 2 and 3). When these chromosomes initially attempted congression, many failed and returned to the spindle pole. Although most chromosomes ultimately aligned on the spindle equator, some required multiple attempts to finally reach the metaphase plate (Videos 2 and 3). In addition, the majority of cells injected with GFP-CEN had defects in alignment, which ranged from cells entering anaphase A in the presence of unaligned chromosomes (28% of cells; Video 3), to cells whose chromosomes aligned but exhibited high oscillations across the metaphase plate (44% of cells). Similar to disruption of MCAK in CHO cells (Maney *et al.*, 1998), 28% of cells had lagging chromosomes and/or chromatids at anaphase that remained at the spindle equator until cytokinesis forced them into one of the two daughter cells (Figure 5B; Videos 2 and 3). Interestingly, we found that although the gross spindle morphology of GFP-CEN-injected cells seemed normal, the distance between spindle poles at each stage of mitosis was decreased compared with uninjected and injected controls (Table 3). The final spindle length in GFP-CEN-injected cells was reduced by 2.9 μ m (19%) compared with control injected cells at the transition between metaphase and anaphase A (*p* < 0.001).

To determine whether these defects were specific to PtK2 cells, we injected prophase *Xenopus* S3 cells and then fixed and stained cells at 40 min postinjection to analyze both the morphology and timing of mitosis (*n* = 35 GFP' and 30 GFP-CEN-injected cells; Supplementary Figures 2 and 3). GFP-CEN bound centromeres in S3s similarly to PtK2s, with the most intense binding at inner kinetochores and variable binding at centromeres (Supplementary Figure 2). Compared with spindles in GFP'-injected cells, GFP-CEN-injected cells displayed normal MT morphology; however, 41% of the prometaphase spindles in GFP-CEN-injected cells exhibited high levels of chromosomes remaining at the poles. We found that at 40 min postinjection, 73% of GFP-CEN-injected S3 cells were still in prometaphase, whereas only 26% of control GFP'-injected S3 cells were in prometaphase (Supplementary Figure 3). The majority of GFP'-injected cells (54%) were already in anaphase and telophase at this time point, indicating that GFP-CEN injection into S3 cell delays chromosome alignment. As a control, we also performed a fixed time-point analysis of PtK2 cells after injection of GFP' or GFP-CEN (*n* = 69 GFP' and 85 GFP-CEN-injected cells). Consistent with our time-lapse data, PtK2s displayed a delay in chromosome alignment, demonstrating that our fixed time-point assay can detect delays in the timing of mitosis specific to GFP-CEN. We also inspected *Xenopus* S3 cells for defects in chromosome segregation due

Table 3. Morphological analysis of time-lapse mitosis in GFP' versus GFP-CEN-injected cells

Observed phenotypes	Control GFP'-injected cells	GFP-CEN-injected cells
Alignment defects	(% cells)	(% cells)
Chromosomes lingering at poles	0	44.4
Multiple attempts to congress	0	55.6
Bad alignment with high oscillations	6.7	27.8
Not all chromosomes congress before anaphase	0	27.8
Total % cells with alignment defects	6.7	89.9
Segregation defects	(% cells)	(% cells)
Lagging chromosomes and/or chromatids	0	27.8
Total % cells with segregation defects	0	27.8
Pole to pole distance measurements	(avg. μ m \pm SEM)	(avg. μ m \pm SEM)
At last chromosome begins congression	16.5 \pm 0.5	14.9 \pm 0.6
At metaphase alignment	15.7 \pm 0.4	13.5 \pm 0.6
At frame before anaphase A onset	15.6 \pm 0.5	12.7 \pm 0.6
Sample size (no. cells)	15	18

Alignment and segregation defects were analyzed in cells injected with control GFP' fusion protein versus GFP-CEN, the centromere dominant-negative version of MCAK. To measure the pole to pole distance, positions of the spindle poles were inferred from the pattern that develops from the clearing of organelles and vesicles from the area of the mitotic spindle.

Table 4. Analysis of chromosome behavior in GFP' versus GFP-CEN-injected cells

Measurement	Control GFP'-injected cells	GFP-CEN-injected cells	Student's <i>t</i> test	Trends
Antipoleward rate during congression ($\mu\text{m}/\text{min}$)	avg. \pm SEM (n) 1.69 \pm 0.16 (23)	avg \pm SEM (n) 1.64 \pm 0.09 (33)	$p = 0.76$	No change
Poleward rate during congression ($\mu\text{m}/\text{min}$)	1.76 \pm 0.13 (23)	1.72 \pm 0.16 (33)	$p = 0.95$	No change
Time in antipoleward motion during congression (%)	96.5 \pm 2.0 (23)	80.9 \pm 3.0 (33)	$p < 0.001$	12% decrease
Time in poleward motion during congression (%)	1.0 \pm 0.1 (23)	10.3 \pm 2.4 (33)	$p < 0.001$	10-fold increase
Oscillation rate at the equator ($\mu\text{m}/\text{min}$)	1.55 \pm 0.21 (10)	1.79 \pm 0.19 (13)	$p = 0.08$	No change
No. switches between AP and P movement during oscillations	2.6 \pm 0.4 (10)	4.2 \pm 0.5 (13)	$p < 0.05$	63% increase
Chromatid mass anaphase A segregation rate ($\mu\text{m}/\text{min}$)	2.06 \pm 0.19 (22)	2.05 \pm 0.14 (30)	$p = 0.32$	No change
Chromatid mass anaphase B segregation rate ($\mu\text{m}/\text{min}$)	1.22 \pm 0.10 (22)	1.12 \pm 0.07 (30)	$p < 0.05$	8% decrease
Pole-pole anaphase A separation rate ($\mu\text{m}/\text{min}$)	0.70 \pm 0.09 (22)	0.63 \pm 0.11 (30)	$p = 0.50$	No change
Pole-pole anaphase B separation rate ($\mu\text{m}/\text{min}$)	1.00 \pm 0.09 (22)	0.80 \pm 0.07 (30)	$p < 0.01$	20% decrease

Chromosome behavior was analyzed in cells injected with control GFP' fusion protein or GFP-CEN according to MATERIALS AND METHODS. Sample sizes for all congression and metaphase oscillation measurements are given in number of chromosomes. Sample sizes for anaphase measurements are given in number of chromatid masses or number of spindle poles analyzed.

to binding of GFP-CEN (Supplementary Figure 4). We found lagging chromosomes and/or chromatin bridges stretched across the spindle equator in 48% of S3 cells in anaphase or telophase ($n = 21$). This defect was observed in only one control injected cell ($n = 19$). Together, our studies in PtK2 and S3 cells demonstrate that multiple cell lines are vulnerable to chromosome alignment and segregation defects upon disruption of MCAK at centromeres. For the remainder of our analyses, we focused on PtK2s because many aspects of mitosis have been well defined in these cells.

Depletion of Centromeric MCAK Perturbs Directionality of Chromosome Movement, but Not Motility Rates

To determine what aspects of chromosome motility were perturbed upon depletion of centromeric MCAK in PtK2 cells, we analyzed individual chromosome behavior in GFP'

versus GFP-CEN-injected cells (Table 4). Although the rates of poleward (P) and antipoleward (AP) movement during chromosome congression were similar, chromosomes in GFP-CEN-injected cells showed a 10-fold increase in the percentage of time moving back to the pole during congression, which was due to an increase in switching between AP and P motion. Overall, these chromosomes took nearly twice as long to congress to the spindle equator. During metaphase, chromosomes in GFP-CEN-injected cells oscillated at similar rates to control chromosomes; however, a subset of chromosomes in GFP-CEN-injected cells exhibited increased frequency of switching between P and AP. These chromosomes traveled farther during each oscillation and oscillated for longer periods of time overall. The rate of chromatid movement and the pole separation rate during anaphase A were also unchanged upon injection of GFP-

Table 5. Measurements of centromere stretch in control GFP' versus GFP-CEN-injected mitotic cells

Mitotic stage	Interkinetochore distance in GFP'-injected cells	Interkinetochore distance in GFP-CEN-injected cells	Student's <i>t</i> test	Trends
Prophase	avg. $\mu\text{m} \pm$ SEM (n) 1.52 \pm 0.04 (24)	avg. $\mu\text{m} \pm$ SEM (n) 1.42 \pm 0.07 (19)	$p = 0.22$	No change
Prometaphase				
Chrom at the pole	2.37 \pm 0.21 (10)	1.51 \pm 0.14 (16)	$p < 0.01$	36% decrease
Bioriented chrom	3.05 \pm 0.09 (42)	2.54 \pm 0.06 (86)	$p < 0.01$	17% decrease
Metaphase	2.96 \pm 0.09 (40)	2.63 \pm 0.07 (37)	$p < 0.01$	11% decrease

chrom, chromosomes.

Interkinetochore distance was determined in GFP' or GFP-CEN-injected cells by measuring the distance from the outer edge of CREST staining at one kinetochore to outer edge of CREST staining at its sister kinetochore. Sample sizes for all interkinetochore measurements are given in number of chromosomes.

CEN; however, GFP-CEN-injected cells exhibited a slight decrease in chromatid and pole separation rates during anaphase B. These results reveal that the predominant defect resulting from depletion of centromeric MCAK is increased frequency of switching between AP and P movement, whereas the rate of chromosome motility is unchanged.

Depletion of Centromere-bound MCAK Decreases Centromere Stretch

To investigate further the defects produced by depleting MCAK from the centromere, we immunostained GFP' or GFP-CEN-injected PtK2 cells with CREST to measure the extent of centromere stretch (Table 5). During prophase, GFP-CEN binding to centromeres resulted in no change in the interkinetochore distance compared with GFP'-injected controls; however, during prometaphase this distance was decreased by 36% on chromosomes located at the spindle poles and by 17% on bioriented chromosomes. This suggests that depletion of centromeric MCAK alters the forces that are acting at the centromere of chromosomes. Treating GFP-CEN-injected cells with 10 $\mu\text{g/ml}$ nocodazole for 30 min further decreased the amount of centromere stretch to 1.6 μm ($n = 11$ chromosomes), indicating that the forces governing centromere stretch were not completely abrogated by GFP-CEN. Although prometaphase chromosomes in GFP-CEN-injected cells exhibited decreased centromere stretch, our time-lapse analyses showed that these cells eventually enter anaphase. To determine whether these cells can overcome the reduction in centromere stretch before anaphase segregation, we also measured interkinetochore distances in the subset of GFP-CEN-injected cells with proper metaphase alignment. Even the aligned metaphase chromosomes in GFP-CEN-injected cells exhibited decreased centromere stretch compared with control injected cells (Table 5), suggesting that these cells segregate their chromosomes without achieving the proper extent of centromere stretch.

The Spindle Checkpoint Protein BubR1 Localizes Normally to Kinetochores in GFP-CEN-injected Cells

Despite alignment and centromere stretch defects due to depletion of centromeric MCAK, every cell injected with GFP-CEN attempted anaphase A segregation of chromatids in our time-lapse analyses. To test the possibility that the spindle checkpoint is dysfunctional, we treated GFP-CEN-injected cells with 10 $\mu\text{g/ml}$ nocodazole to depolymerize MTs and found that cells arrested in mitosis with condensed, unsegregated chromosomes for up to 2 h after nocodazole treatment (our unpublished data; $n = 11$ cells). In addition, we immunostained GFP-CEN-injected cells for BubR1, a spindle checkpoint protein that strongly stains the kinetochores of unaligned chromosomes but is significantly reduced at kinetochores on aligned chromosomes (Jablonski *et al.*, 1998; Hoffman *et al.*, 2001). We found that cells injected with GFP-CEN were indistinguishable from GFP'-injected control cells for localization of BubR1 in prometaphase and metaphase cells (Figure 6; $n = 10$ GFP-CEN- and 11 GFP'-injected cells). In combination with the mitotic delay exhibited by depletion of centromeric MCAK, these data suggest that GFP-CEN-injected cells may have a functional spindle checkpoint. This, in turn, implies that the misaligned chromosomes typical of these cells are not detected by the checkpoint, although further experimentation will be required to resolve this issue.

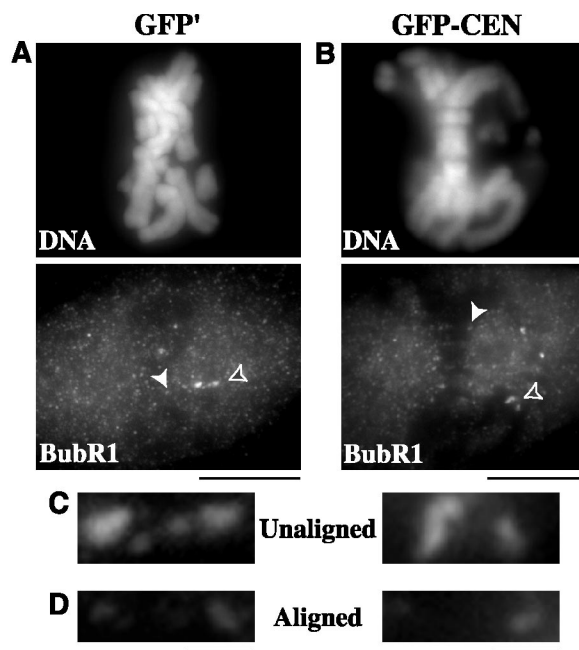


Figure 6. BubR1 stains kinetochores of unaligned chromosomes but not aligned chromosomes in GFP-CEN-injected PtK2 cells. BubR1 staining at kinetochores was compared between GFP'-injected control cells (A) and GFP-CEN-injected cells (B). (C) BubR1 staining at kinetochores of unaligned chromosomes is indicated in A and B by open arrowheads. (D) BubR1 staining at kinetochores of aligned chromosomes is indicated in A and B by solid arrowheads. Bars (A and B), 10 μm ; (C and D), 1 μm .

Depletion of Centromeric MCAK Leads to Severe Segregation Defects

By using immunofluorescence microscopy, we found that GFP-CEN-injected cells had even more pronounced defects in chromosome segregation than our phase contrast analysis indicated. Overall, 44% of GFP-CEN-injected cells had mis-segregated chromosomes ($n = 75$; Figure 7, A–F). 35% of all GFP-CEN-injected cells exhibited lagging chromatids (Figure 7, A and B), and 7% exhibited lagging chromosomes (Figure 7C), which together equated to a 19-fold increase over control cells ($n = 46$). In addition, 25% of GFP-CEN-injected cells showed gross missegregations in the amount of DNA at one pole versus the other (Figure 7, B and D), which was increased fourfold over controls. To inspect these segregation defects more closely, we examined CREST staining in GFP-CEN-injected cells. In 50% of GFP-CEN-injected cells ($n = 14$), the number of kinetochores segregated to one pole was different from the number of kinetochores segregated to the other pole (Figure 7E). In some cells this difference was as high as 12 chromatids. In addition to missegregated chromatids, we noticed that the morphology of the CREST staining was often altered in GFP-CEN-injected cells. All of the lagging chromatids analyzed ($n = 12$) exhibited a stretched CREST morphology compared with the staining pattern of CREST at normally segregated chromatids (Figure 7F). These chromatids were stretched an average of $1.39 \pm 0.17 \mu\text{m}$, which equated to a 1.6- to 4.2-fold increase compared with the normal diameter of CREST (0.52 μm ; $n = 60$) at properly segregated kinetochores in anaphase ($p < 0.001$). This morphology has been described in detail for lagging chromatids induced by long-term nocodazole treatment and subsequent washout in PtK cells (Cimini

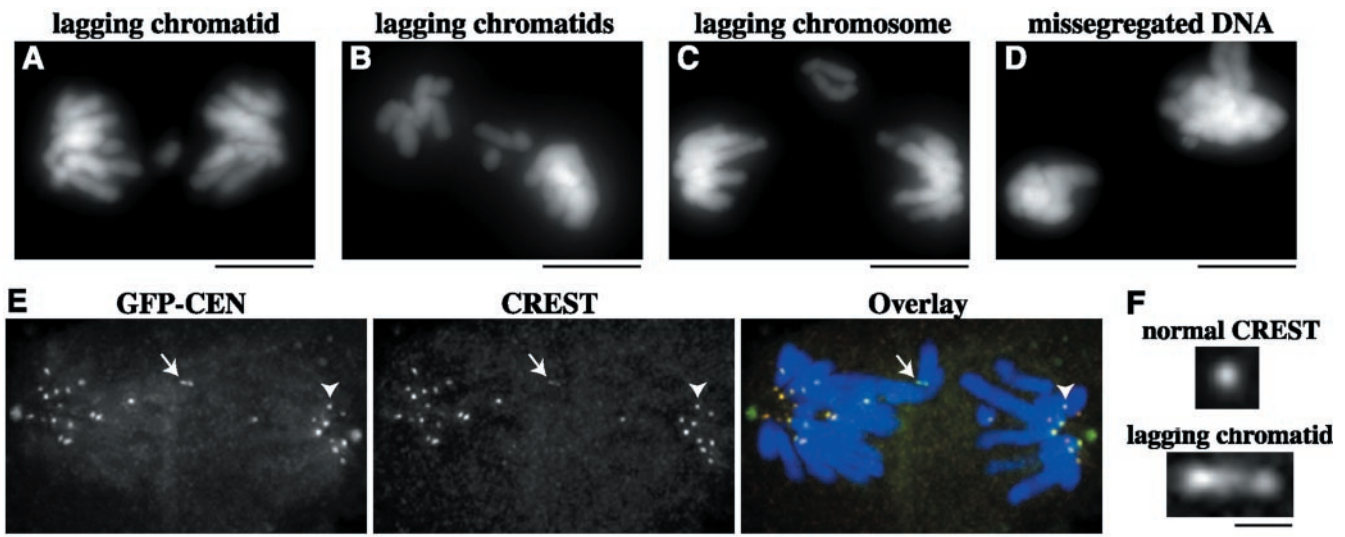


Figure 7. Depletion of centromere-bound MCAK leads to severe chromosome missegregation. PtK2 cells in prophase were injected with GFP-CEN and processed for fluorescence microscopy of DNA at 40 min postinjection. Segregation defects in GFP-CEN-injected cells included (A and B) lagging chromatids during anaphase and telophase, (C) lagging chromosomes during anaphase, as well as (B and D) grossly missegregated amounts of DNA. (E and F) GFP-CEN-injected cells were fixed and immunostained for CREST and DNA at 40 min postinjection. (E) GFP-CEN-injected cell with lagging chromatid (white arrow) and missegregated DNA in anaphase B. CREST staining shows that 17 chromatids were segregated to the left pole, whereas 11 chromatids were segregated to the right pole. (F) The CREST staining pattern of the lagging chromosome (bottom) is stretched threefold compared with CREST at a normally segregated chromatid (top), indicated by arrowhead in E. Bars (A-E), 10 μm ; (F), 1 μm .

et al., 2001) and is indicative of merotelic kinetochore attachments. Overall, these data demonstrate that depletion of centromere-bound MCAK leads to severe missegregation of DNA in mitosis, despite the finding that anaphase timing and chromatid motility rates are normal. These data also suggest that the lagging chromosomes resulting from depletion of centromeric MCAK are caused by merotelic attachments at kinetochores formed before anaphase and not because MCAK is the anaphase A depolymerase in cells.

Depletion of Centromeric MCAK Leads to Improper Kinetochore–Microtubule Attachments

Our observations of delayed chromosome congression, lagging chromosomes, and decreased centromere stretch in GFP-CEN-injected cells suggest that depletion of centromeric MCAK results in abnormal interactions between the kinetochores and MTs. To examine the ultrastructural characteristics of kinetochore–MT attachments in these cells, we used correlative light/serial-section EM (Khodjakov *et al.*, 1997; Rieder and Cassels, 1999). We injected GFP-CEN into prophase cells and followed the fate of injected cells by phase contrast time-lapse microscopy. Cells were then fixed and processed for transmission EM to examine centrosome, K-fiber, and kinetochore morphology during specific chromosome behavior (Figure 8). The ultrastructure of spindle poles in prometaphase, metaphase, and anaphase were normal in GFP-CEN-injected cells (Figure 8C). We analyzed two late prometaphase/metaphase cells that had most chromosomes aligned on the spindle equator as well as several chromosomes that were delayed in congression and were stably positioned at the poles (Video 4). We found that the overall organization of the centromere region, including the kinetochore trilaminar plate, was normal for properly aligned chromosomes (Figure 8, A and B; $n = 10$ kinetochores). Kinetochores were positioned on the opposite sides of the primary constriction and interacted with MTs in a typical end-on manner. K-fibers approached kinetochores at

an angle of $\sim 90^\circ$. Most MTs terminated within the outer layer of the kinetochore, although sometimes they penetrated deeper toward the inner layer. In contrast, the organization of the centromere region of chromosomes that were “stuck” at spindle poles during prometaphase was severely abnormal, although the kinetochore trilaminar plate was preserved (Figure 8, C–K; $n = 6$ kinetochores). Specifically, sister kinetochores were positioned on the same side of the primary constriction and sometimes faced away from the proximal pole. Such orientation is extremely unusual for mono-oriented chromosomes (Roos, 1973; Cassimeris *et al.*, 1994). MTs approached these kinetochores at very shallow angles, practically running parallel to the surface of the kinetochore plate. Serial-section reconstruction of one such chromosome revealed that both kinetochores had several MTs that emanated from the kinetochore toward both the proximal and distal poles at the same time (Figure 8K). Thus, each individual kinetochore of this chromosome was merotelically oriented (connected to both spindle poles), whereas the chromosome as a whole was also syntelic (as both sister kinetochores were simultaneously connected to the same pole).

We also analyzed a cell that initiated anaphase in the presence of chromosomes that were stuck at the spindle poles (Video 5). This cell was fixed ~ 10 s after anaphase onset as the chromatids were separating from each other. As expected, kinetochores of the chromosomes that had aligned properly before anaphase had normal morphology. Unfortunately, the orientation of the kinetochores on the unaligned chromosome (parallel to the EM sectioning plane) did not allow us to reveal fine structural details of kinetochore–MT interactions, but it was clear that both of these kinetochores were connected to the same spindle pole, i.e., the chromosome was syntelic before anaphase onset (our unpublished data). These results clearly demonstrate that depletion of centromeric MCAK leads to a variety of defective interactions between kinetochores and MTs, including merotelic, syntelic, and combined merotelic-syntelic kinetochore–MT attachments.

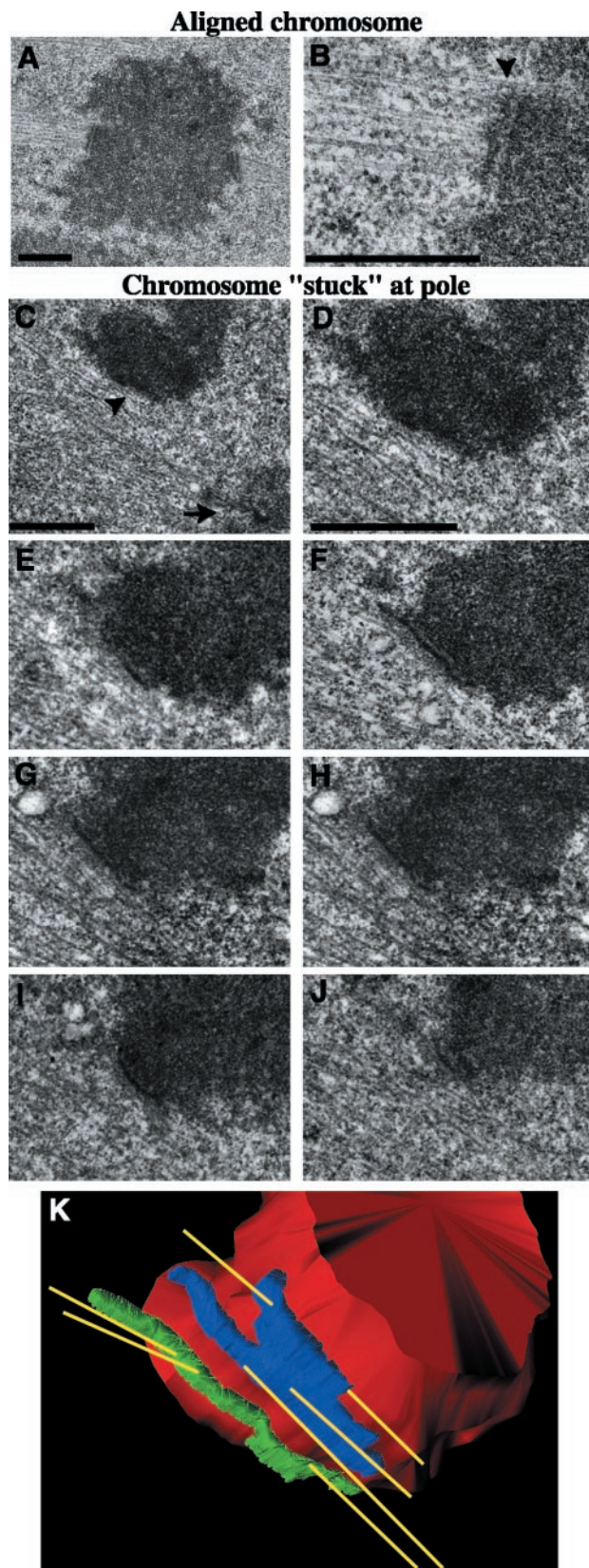


Figure 8. Centromeric MCAK depletion leads to improper kinetochore-microtubule attachments in PtK2 cells. Correlative light/serial-section EM was performed on GFP-CEN-injected cells to analyze kinetochore and K-fiber morphology. Low-magnification

DISCUSSION

MCAK Centromere Localization Is Altered by Microtubule Attachment and Tension

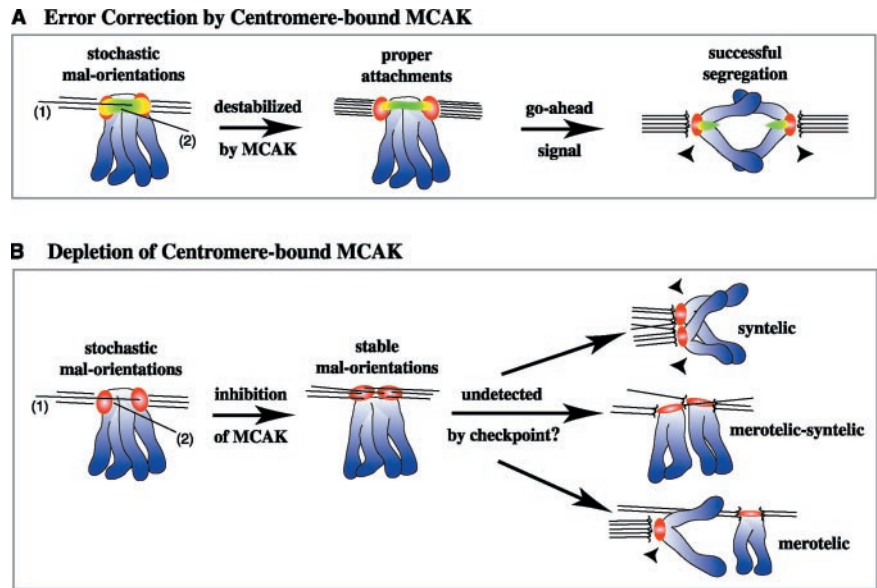
We found that MCAK displays differential centromere localization that is responsive to MT attachment and tension generated across the centromere. Under conditions of low tension, MCAK extends farther toward the kinetochore inner plate and thus closer to MT binding sites. During metaphase, when the centromere is under high levels of tension, MCAK is predominantly centromeric. Interestingly, the reduction of MCAK at the inner kinetochore plate during metaphase correlates with measurements of K-fiber stability, which have demonstrated that high levels of tension enhance the stability of preexisting kinetochore MTs and increase the number of MTs in the K-fiber (King and Nicklas, 2000; McIntosh *et al.*, 2002). These observations suggest that MCAK is moved away from attached kinetochore MTs as tension is established, an idea that is supported by our data that MCAK is enriched at the leading kinetochore of congressing chromosomes. In PtK cells, the leading kinetochore is only attached to one to eight depolymerizing MTs, whereas the trailing kinetochore has nearly a full complement of MTs (McEwen *et al.*, 1997), suggesting that MCAK is enriched in the kinetochore regions with fewer MT attachments. It is not clear what controls MCAK relocalization, but it may be sensitive to chemical changes, such as phosphorylation, that take place at the leading kinetochore (Gorbsky and Ricketts, 1993; Nicklas *et al.*, 1995). Later in mitosis, MT attachment also plays a role in excluding MCAK from the inner plate of the kinetochore in anaphase. Although centromere tension is released upon degradation of cohesins between sister chromatids, the number of MTs in the K-fiber is at its highest during anaphase A (McEwen *et al.*, 1997).

Depletion of Centromere-bound MCAK Decreases Centromere Stretch

The relocalization of MCAK from inner kinetochores to centromeres may be correlated with a role in maintaining centromere tension because depletion of centromeric MCAK led to a 17–36% reduction in interkinetochore distances in prometaphase cells. Our EM analysis offers an explanation for why the interkinetochore distances were dramatically lower for chromosomes located at the poles. The kinetochores of these chromosomes were positioned on the same side of the primary constriction with improper merotelic-syntelic MT attachments, which would not allow for centromere stretching. Intriguingly, aligned chromosomes that established proper amphitelic (bioriented), end-on attachments to the mitotic spindle also exhibited decreased interkinetochore distances. One potential explanation for this effect is that depletion of centromere-bound MCAK affects the flexibility

(A) and high-magnification (B) images of an aligned chromosome with normal kinetochore morphology and MT attachments; arrowhead is positioned at the kinetochore-MT interface. (C) Low-magnification image of a chromosome that remained for an extended period of time at the pole during mitosis. Arrow denotes a centrosome; arrowhead denotes a kinetochore. (D–J) High-magnification, 100-nm serial-section images of the chromosome shown in C reveal that both kinetochores are attached to MTs emanating from both poles, which makes this chromosome both merotelically and syntelically oriented on the spindle. (K) The 3-D structure of MTs attached to the merotelic-syntelic kinetochores of the chromosome shown in C–J. The chromosome is shown in red, MTs in yellow, and sister kinetochores in blue and green. Bars, 1 μ m.

Figure 9. Model for destabilization of mal-oriented kinetochore–microtubule attachments by centromere-bound MCAK. Chromosomes are in blue, CREST is in red, MCAK is in green, and MCAK colocalized with CREST is in yellow. (A) Maloriented MT attachments, such as kinetochore MTs penetrating past the outer kinetochore (1) or nonkinetochore MTs invading the centromere (2) are depolymerized upon encountering MCAK. This allows for turnover and the eventual formation of properly oriented attachments. The spindle checkpoint gives the go-ahead signal, and proper segregation is achieved. (B) On depletion of centromere-bound MCAK, however, maloriented attachments are not destabilized. Stable mal-orientations (such as merotelic and/or syntelic kinetochore–MT attachments) are not resolved, and missegregation of chromatids occurs at anaphase.



of the centromere. This explanation is unlikely; our EM data of the “near-pole” chromosomes reveal that sister kinetochores can easily shift their positions, indicating that the MCAK-depleted centromeres remain flexible. Another possibility for the reduction in the centromere stretch is that depletion of centromeric MCAK affects MT dynamics of the K-fiber. It has been shown that chromosomes display reduced centromere stretch under conditions that reduce MT dynamics, e.g., hypothermia (Shannon *et al.*, 2002) or paclitaxel (Waters *et al.*, 1996a). Finally, these results may indicate that the depolymerase activity of MCAK is needed to generate tension across the centromere. Although we currently lack decisive data to support or disprove this hypothesis, it has important implications for our understanding of MCAK function and should be tested directly in the future.

MCAK Is Required for Proper Congression of Chromosomes

Our findings of mitotic delay, alignment defects, and chromosome missegregation upon depletion of centromeric MCAK are generally consistent with studies in other systems, demonstrating the importance of Kin Is in chromosome positioning. Perturbation of MCAK in mammalian CHO cells and mutations in the orthologues Klp5 and Klp6 in *S. pombe* both lead to delays in mitosis, with the fission yeast mutants exhibiting defects in chromosome congression and alignment (Maney *et al.*, 1998; Garcia *et al.*, 2002; West *et al.*, 2002). In addition, depletion of centromere-bound MCAK in metaphase-arrested *Xenopus* egg extracts causes chromosomes to misalign at the spindle equator (Walczak *et al.*, 2002). Upon depletion of centromeric MCAK in our assays, the rates of chromosome movement were normal during all stages of mitosis. In particular, our findings of normal rates of chromatid to pole movement in GFP-CEN-injected cells argue against the idea that MCAK is required to move chromosomes poleward during anaphase A. Rather, our data are consistent with the idea that MCAK is required before anaphase to promote proper attachment of chromosomes to the spindle; thus, when MCAK at the centromere is depleted, defective attachments formed preanaphase are not resolved, leading to segregation defects at anaphase.

Additional support for this model comes from our data showing that many aspects of chromosome behavior are

perturbed during congression. Chromosomes were delayed in the initiation of congression to the metaphase plate, which could be due to improper K-fiber attachments, such as those demonstrated for chromosomes stuck at the poles during prometaphase and anaphase. During congression, chromosomes exhibited a considerable increase in the frequency of switching between P and AP motion, which may indicate that MCAK is required for coordination of sister kinetochore activity. Alternatively, the decrease in centromere stretch upon depletion of centromeric MCAK may have disabled tension-sensitive mechanisms that direct chromosome movement (Skibbens *et al.*, 1993; Skibbens and Salmon, 1997) and/or tension-sensitive switching between depolymerization and polymerization of MT plus ends at the kinetochore (Maddox *et al.*, 2003). Interestingly, the aberrant chromosome movement in GFP-CEN-injected cells is reminiscent of the chromosome fragments containing a single kinetochore produced by laser cutting in PtK cells (Khodjakov *et al.*, 1997), suggesting that some of the defects during congression could be attributed to the merotelic attachments resulting from centromeric MCAK depletion.

MCAK Is Required to Destabilize Improper Kinetochore–Microtubule Attachments during Mitosis

Many naturally occurring and induced errors in chromosome orientation on the mitotic spindle involve improper attachment of MTs to chromosomes. The ultimate goal of chromosome biorientation can be thwarted by the presence of MTs binding at inappropriate sites, such as the centromere (Rieder, 1982). Even MTs attaching at the correct binding sites in the outer plate of the kinetochore can be blamed for missegregation of chromosomes at anaphase, such as chromosomes with syntelic or merotelic attachments. Despite the type of malorientation, resolution requires elimination of the inappropriately attached MT and substitution with a properly positioned kinetochore MT. MT attachment turnover has been linked to interkinetochore tension in both budding yeast mitosis (Tanaka, 2002) and grasshopper spermatid meiosis (Nicklas, 1997), such that kinetochore–MT attachments are unstable in conditions of low tension and stable in conditions of high tension. Other reports suggest that low tension enables error correction by promoting re-

lease of improperly attached MTs from the spindle pole and/or by promoting phosphorylation of kinetochore components (Nicklas, 1997).

Our data suggest that the subpopulation of MCAK localized at the centromere may be involved in both error prevention and error correction. The process of error prevention would be especially important during the early stages of mitosis when MTs are probing the three-dimensional space of the cell to capture kinetochores. The proximity of MCAK to kinetochores under conditions of low tension may promote MT dynamics at plus ends, thus increasing the chance for correct attachments because a more dynamic MT could undergo more frequent "sampling" for proper binding sites at kinetochores. Consistent with this idea, we previously showed that MCAK stimulates catastrophe and suppresses rescue of MT plus ends in PtK2 cells (Kline-Smith and Walczak, 2002); thus, local stimulation of MT dynamics could be controlled by the positioning of this protein.

Although MCAK is proximal to the kinetochore during conditions of low tension, chromosomes exhibiting high tension leads to sequestration of MCAK to the centromere, which may contribute to the stability of properly attached MTs. The localization and activity of centromeric MCAK are also consistent with its involvement in error correction in a mature K-fiber, leading us to propose the following model (Figure 9). As mature K-fibers turn over during later mitosis, the occasional nonkinetochore MT invading the centromere or kinetochore MT penetrating past the kinetochore is destroyed upon encountering an MT depolymerase at the centromere (Figure 9A). Consistent with this idea, improper MT attachments are usually unstable and are corrected during mitosis (Rieder and Salmon, 1998; Cimini *et al.*, 2003). Upon depletion of centromeric MCAK, however, destabilization of improperly positioned MTs is suppressed, leading to stable merotelic and/or syntelic attachment defects before anaphase (Figure 9B). Upon initiation of anaphase A, these defective MT attachments lead to various segregation defects, such as lagging chromosomes and chromatids, as well as full chromosomes that are segregated to the same spindle pole. Overall, these data suggest a surprisingly simple mechanism to both prevent and correct malorientations by the tension- and MT attachment-sensitive localization of a MT depolymerase at the centromere. Alternatively, our findings could indicate that MCAK is required during early mitosis to resolve lateral MT associations at kinetochores into proper end-on attachments. In addition, if MCAK is used to generate tension across centromeres, then the decrease in centromere stretch seen in GFP-CEN-injected cells may indirectly increase the frequency with which improper attachments are made at kinetochores. We think this is unlikely, as similar decreases in centromere stretch in PtKs under hypothermic conditions do not lead to improper kinetochore-MT attachments (Cassimeris *et al.*, 1990; Wise *et al.*, 1991; Shannon *et al.*, 2002).

Recent studies in *Xenopus* egg extracts have characterized a new inner centromeric protein called ICIS, which stimulates MCAK-dependent MT depolymerization *in vitro* (Ohi *et al.*, 2003). Because ICIS is localized to both the inner centromere and to nonkinetochore MTs associated laterally with the centromere, it may interact with MCAK to destabilize deleterious MT attachments in the inner centromere to prevent missegregation. This model is in agreement with our findings of multiple attachment defects upon depletion of MCAK at centromeres. In addition, many recent studies have focused on the ability of an inner centromere protein kinase, Ipl1p/Aurora B, to correct improper kinetochore-MT attachments (Biggins *et al.*, 1999; Shannon and

Salmon, 2002; Ditchfield *et al.*, 2003; Hauf *et al.*, 2003). Because Aurora B has not been shown to directly destabilize MTs, an enticing possibility is that Aurora B phosphorylates MCAK to regulate its MT depolymerase activity and/or centromere localization.

Despite the presence of maloriented kinetochore-MT attachments upon depletion of centromeric MCAK, none of the cells we observed underwent mitotic arrest. It is not surprising that merotelically oriented chromatids were not sensed by the checkpoint, as is the case in other cultured cells (Cimini *et al.*, 2001, 2002); however, we also saw full chromosomes remaining at the poles upon anaphase A onset. Therefore, it is possible that centromeric MCAK depletion has abolished assembly of the kinetochore, leading to a malfunctioning checkpoint, or that MCAK itself plays a role in the checkpoint pathway. Our findings of normal kinetochore trilaminar plate ultrastructure, normal CREST (CENP-A, -B, and -C) staining at the inner kinetochore region, normal CENP-E staining at the outer kinetochore region, and the positionally sensitive localization of BubR1 in our injected cells suggest this is not the case. On GFP-CEN injection, cells were delayed in mitosis, which requires an active checkpoint. In addition, injection of our centromere dominant-negative protein followed by nocodazole treatment led to a mitotic arrest, suggesting that the spindle checkpoint is functioning upon the loss of K-fiber attachments in these cells.

Alternatively, it is possible that depletion of MCAK at the centromere leads to subtle defects in the spindle checkpoint that inhibit the detection of improper MT attachments and/or perturb BubR1 binding at centromeres exhibiting decreased stretch. Clearly, additional work is required to determine whether centromeric MCAK depletion slightly alters the spindle checkpoint or whether the myriad of mal-oriented kinetochore-MT attachments in GFP-CEN-injected cells are not sensed by a functional checkpoint in PtK cells. Interestingly, recent work in PtK cells has demonstrated that mechanisms exist both before and during anaphase to correct improper kinetochore-MT attachments and ensure proper segregation of DNA (Cimini *et al.*, 2003). Our work suggests that MT depolymerization by centromere-bound MCAK plays an important role in this active process of error correction in mitotic cells.

ACKNOWLEDGMENTS

We thank Tarun Kapoor, Tim Yen, Bill Brinkley, and Guowei Fang for reagents, Duane Compton and Michael Gordon for technical assistance, and the Salmon lab for providing Rose chambers. In addition, we are indebted to Ted Salmon, Arshad Desai, Ryoma (Puck) Ohi, and Gary Gorbisky for helpful discussion and ideas, as well as Sue Biggins, Sarah Johnstone, and David Hedrick for comments on the manuscript. Electron microscopy was performed at the Wadsworth Center's EM core facility. This work was funded by grants from the NIH to CEW and AK, and by a grant from the AHA to SKS. CEW is a Scholar of the Leukemia and Lymphoma Society.

REFERENCES

- Biggins, S., Severin, F.F., Bhalla, N., Sassoan, I., Hyman, A.A., and Murray, A.W. (1999). The conserved protein kinase Ipl1 regulates microtubule binding to kinetochores in budding yeast. *Genes Dev.* 13, 532-544.
- Cassimeris, L., Rieder, C.L., Rupp, G., and Salmon, E.D. (1990). Stability of microtubule attachment to metaphase kinetochores in PtK1 cells. *J. Cell Sci.* 96, 9-15.
- Cassimeris, L., Rieder, C.L., and Salmon, E.D. (1994). Microtubule assembly and kinetochore directional instability in vertebrate monopolar spindles: implications for the mechanism of chromosome congression. *J. Cell Sci.* 107, 285-297.

- Cimini, D., Howell, B., Maddox, P., Khodjakov, A., Degraffi, F., and Salmon, E.D. (2001). Merotelic kinetochore orientation is a major mechanism of aneuploidy in mitotic mammalian tissue cells. *J. Cell Biol.* 153, 517–527.
- Cimini, D., Fioravanti, D., Salmon, E.D., and Degraffi, F. (2002). Merotelic kinetochore orientation versus chromosome mono-orientation in the origin of lagging chromosomes in human primary cells. *J. Cell Sci.* 115, 507–515.
- Cimini, D., Moree, B., Canman, J.C., and Salmon, E.D. (2003). Merotelic kinetochore orientation occurs frequently during early mitosis in mammalian tissue cells and error correction is achieved by two different mechanisms. *J. Cell Sci.* 116, 4213–25.
- Cohen, M.W., Hoffstrom, B.G., and DeSimone, D.W. (2000). Active zones on motor nerve terminals contain alpha 3beta 1 integrin. *J. Neurosci.* 20, 4912–4921.
- De Brabander, M., Geuens, G., De Mey, J., and Joniau, M. (1981). Nucleated assembly of mitotic microtubules in living PTK2 cells after release from nocodazole treatment. *Cell Motil.* 1, 469–483.
- Desai, A., Verma, S., Mitchison, T.J., and Walczak, C.E. (1999). Kin I kinesins are microtubule-destabilizing enzymes. *Cell.* 96, 69–78.
- Ditchfield, C., Johnson, V.L., Tighe, A., Ellston, R., Haworth, C., Johnson, T., Mortlock, A., Keen, N., and Taylor, S.S. (2003). Aurora B couples chromosome alignment with anaphase by targeting BubR1, Mad2, and Cenp-E to kinetochores. *J. Cell Biol.* 161, 267–280.
- Garcia, M.A., Koonrugsa, N., and Toda, T. (2002). Two kinesin-like Kin I family proteins in fission yeast regulate the establishment of metaphase and the onset of anaphase A. *Curr. Biol.* 12, 610–621.
- Gorbsky, G.J., and Ricketts, W.A. (1993). Differential expression of a phosphoprotein at the kinetochores of moving chromosomes. *J. Cell Biol.* 122, 1311–1321.
- Gordon, M.B., Howard, L., and Compton, D.A. (2001). Chromosome movement in mitosis requires microtubule anchorage at spindle poles. *J. Cell Biol.* 152, 425–434.
- Goshima, G., and Vale, R.D. (2003). The roles of microtubule-based motor proteins in mitosis: comprehensive RNAi analysis in the *Drosophila* S2 cell line. *J. Cell Biol.* 162, 1003–16.
- Hauf, S., Cole, R.W., LaTerra, S., Zimmer, C., Schnapp, G., Walter, R., Heckel, A., Van Meel, J., Rieder, C.L., and Peters, J.M. (2003). The small molecule Hesperadin reveals a role for Aurora B in correcting kinetochore-microtubule attachment and in maintaining the spindle assembly checkpoint. *J. Cell Biol.* 161, 281–294.
- Hoffman, D.B., Pearson, C.G., Yen, T.J., Howell, B.J., and Salmon, E.D. (2001). Microtubule-dependent changes in assembly of microtubule motor proteins and mitotic spindle checkpoint proteins at PtK1 kinetochores. *Mol. Biol. Cell.* 12, 1995–2009.
- Hunter, A.W., Caplow, M., Coy, D.L., Hancock, W.O., Diez, S., Wordeman, L., and Howard, J. (2003). The kinesin-related protein MCAK is a microtubule depolymerase that forms an ATP-hydrolyzing complex at microtubule ends. *Mol. Cell.* 11, 445–457.
- Inoue, S., and Salmon, E.D. (1995). Force generation by microtubule assembly/disassembly in mitosis and related movements. *Mol. Biol. Cell.* 6, 1619–1640.
- Jablonski, S.A., Chan, G.K., Cooke, C.A., Earnshaw, W.C., and Yen, T.J. (1998). The hBUB1 and hBUBR1 kinases sequentially assemble onto kinetochores during prophase with hBUBR1 concentrating at the kinetochore plates in mitosis. *Chromosoma* 107, 386–396.
- Kapoor, T.M., Mayer, T.U., Coughlin, M.L., and Mitchison, T.J. (2000). Probing spindle assembly mechanisms with monastrol, a small molecule inhibitor of the mitotic kinesin, Eg5. *J. Cell Biol.* 150, 975–988.
- Khodjakov, A., Cole, R.W., McEwen, B.F., Buttle, K.F., and Rieder, C.L. (1997). Chromosome fragments possessing only one kinetochore can congress to the spindle equator. *J. Cell Biol.* 136, 229–240.
- King, J.M., and Nicklas, R.B. (2000). Tension on chromosomes increases the number of kinetochore microtubules but only within limits. *J. Cell Sci.* 113 Pt 21, 3815–3823.
- Kline-Smith, S.L., and Walczak, C.E. (2002). The microtubule-destabilizing kinesin XKCM1 regulates microtubule dynamic instability in cells. *Mol. Biol. Cell.* 13, 2718–2731.
- Maddox, P., Straight, A., Coughlin, P., Mitchison, T.J., and Salmon, E.D. (2003). Direct observation of microtubule dynamics at kinetochores in *Xenopus* extract spindles: implications for spindle mechanics. *J. Cell Biol.* 162, 377–382.
- Maney, T., Hunter, A.W., Wagenbach, M., and Wordeman, L. (1998). Mitotic centromere-associated kinesin is important for anaphase chromosome segregation. *J. Cell Biol.* 142, 787–801.
- Marko, M., and Leith, A. (1996). Stereocon—three-dimensional reconstructions from stereoscopic contouring. *J. Struct. Biol.* 116, 93–98.
- McEwen, B.F., Heagle, A.B., Cassels, G.O., Buttle, K.F., and Rieder, C.L. (1997). Kinetochore fiber maturation in PtK1 cells and its implications for the mechanisms of chromosome congression and anaphase onset. *J. Cell Biol.* 137, 1567–1580.
- McIntosh, J.R., Grishchuk, E.L., and West, R.R. (2002). Chromosome-microtubule interactions during mitosis. *Annu. Rev. Cell Dev. Biol.* 18, 193–219.
- Musacchio, A., and Hardwick, K.G. (2002). The spindle checkpoint: structural insights into dynamic signalling. *Nat. Rev. Mol. Cell. Biol.* 3, 731–41.
- Nicklas, R.B., Ward, S.C., and Gorbsky, G.J. (1995). Kinetochore chemistry is sensitive to tension and may link mitotic forces to a cell cycle checkpoint. *J. Cell Biol.* 130, 929–939.
- Nicklas, R.B. (1997). How cells get the right chromosomes. *Science.* 275, 632–637.
- Ohi, R., Coughlin, M.L., Lane, W.S., and Mitchison, T.J. (2003). An inner centromere protein that stimulates the microtubule depolymerizing activity of a Kin I kinesin. *Dev. Cell.* 5, 309–321.
- Ovechkina, Y., and Wordeman, L. (2003). Unconventional motoring: an overview of the kin C and kin I kinesins. *Traffic.* 4, 367–375.
- Rieder, C.L. (1982). The formation, structure, and composition of the mammalian kinetochore and kinetochore fiber. *Int. Rev. Cytol.* 79, 1–58.
- Rieder, C.L., and Cassels, G. (1999). Correlative light and electron microscopy of mitotic cells in monolayer cultures. *Methods Cell Biol.* 61, 297–315.
- Rieder, C.L., and Salmon, E.D. (1998). The vertebrate cell kinetochore and its roles during mitosis. *Trends Cell Biol.* 8, 310–318.
- Roos, U.P. (1973). Light and electron microscopy of rat kangaroo cells in mitosis. II. Kinetochore structure and function. *Chromosoma* 41, 195–220.
- Salmon, E.D., Inoue, T., Desai, A., and Murray, A.W. (1994). High resolution multimode digital imaging system for mitosis studies in vivo and in vitro. *Biol. Bull.* 187, 231–232.
- Shannon, K.B., Canman, J.C., and Salmon, E.D. (2002). Mad2 and BubR1 function in a single checkpoint pathway that responds to a loss of tension. *Mol. Biol. Cell.* 13, 3706–3719.
- Shannon, K.B., and Salmon, E.D. (2002). Chromosome dynamics: new light on Aurora B kinase function. *Curr. Biol.* 12, R458–460.
- Skibbens, R.V., Skeen, V.P., and Salmon, E.D. (1993). Directional instability of kinetochore motility during chromosome congression and segregation in mitotic newt lung cells: a push-pull mechanism. *J. Cell Biol.* 122, 859–875.
- Skibbens, R.V., and Salmon, E.D. (1997). Micromanipulation of chromosomes in mitotic vertebrate tissue cells: tension controls the state of kinetochore movement. *Exp. Cell Res.* 235, 314–24.
- Tanaka, T.U. (2002). Bi-orienting chromosomes on the mitotic spindle. *Curr. Opin. Cell Biol.* 14, 365–371.
- Thrower, D.A., Jordan, M.A., and Wilson, L. (1996). Modulation of CENP-E organization at kinetochores by spindle microtubule attachment. *Cell Motil. Cytoskeleton.* 35, 121–133.
- Walczak, C.E., Mitchison, T.J., and Desai, A. (1996). XKCM1, a *Xenopus* kinesin-related protein that regulates microtubule dynamics during mitotic spindle assembly. *Cell.* 84, 37–47.
- Walczak, C.E., Gan, E.C., Desai, A., Mitchison, T.J., and Kline-Smith, S.L. (2002). The microtubule-destabilizing kinesin XKCM1 is required for chromosome positioning during spindle assembly. *Curr. Biol.* 12, 1885–1889.
- Waters, J.C., Mitchison, T.J., Rieder, C.L., and Salmon, E.D. (1996a). The kinetochore microtubule minus-end disassembly associated with poleward flux produces a force that can do work. *Mol. Biol. Cell.* 7, 1547–1558.
- Waters, J.C., Skibbens, R.V., and Salmon, E.D. (1996b). Oscillating mitotic newt lung cell kinetochores are, on average, under tension and rarely push. *J. Cell Sci.* 109, 2823–2831.
- West, R.R., Malmstrom, T., and McIntosh, J.R. (2002). Kinesins klp5(+) and klp6(+) are required for normal chromosome movement in mitosis. *J. Cell Sci.* 115, 931–940.
- Wise, D., Cassimeris, L., Rieder, C.L., Wadsworth, P., and Salmon, E.D. (1991). Chromosome fiber dynamics and congression oscillations in metaphase PtK2 cells at 23 degrees C. *Cell Motil. Cytoskeleton.* 18, 131–142.
- Wordeman, L., and Mitchison, T.J. (1995). Identification and partial characterization of mitotic centromere-associated kinesin, a kinesin-related protein that associates with centromeres during mitosis. *J. Cell Biol.* 128, 95–104.
- Zhou, J., Yao, J., and Joshi, H.C. (2002). Attachment and tension in the spindle assembly checkpoint. *J. Cell Sci.* 115, 3547–3555.